

Dalton Transactions

Accepted Manuscript



This is an *Accepted Manuscript*, which has been through the Royal Society of Chemistry peer review process and has been accepted for publication.

Accepted Manuscripts are published online shortly after acceptance, before technical editing, formatting and proof reading. Using this free service, authors can make their results available to the community, in citable form, before we publish the edited article. We will replace this *Accepted Manuscript* with the edited and formatted *Advance Article* as soon as it is available.

You can find more information about *Accepted Manuscripts* in the [Information for Authors](#).

Please note that technical editing may introduce minor changes to the text and/or graphics, which may alter content. The journal's standard [Terms & Conditions](#) and the [Ethical guidelines](#) still apply. In no event shall the Royal Society of Chemistry be held responsible for any errors or omissions in this *Accepted Manuscript* or any consequences arising from the use of any information it contains.



Naphthylaminoborane: From structural switches to frustrated Lewis pairs reactivity

Daniel Pla,^{a,*} Omar Sadek,^{a,b} Sarah Cadet,^a Béatrice Mestre-Voegtlé,^a and Emmanuel Gras.^{a,*}

Received 00th January 20xx,
Accepted 00th January 20xx

DOI: 10.1039/x0xx00000x

www.rsc.org/

A series of naphthyl-bridged amino-borane derivatives, namely 1-(dimethylamino)-8-naphthylboranes (**1**, **3**, **5**, **7**) and 5-(dimethylamino)-6-acenaphthylboranes (**2**, **4**, **6**, **8**, **10**, **11**), differing in the steric and electronic properties of the boryl moiety, have been synthesized and fully characterized by spectroscopic and crystallographic means. Structural X-ray analysis of the peri-atom displacement and ring torsion angles served to experimentally assess the presence and magnitude of the B–N interactions. The reversible quaternarization of nitrogen has been explored and was found to provide an efficient switch corresponding to different molecular organizations. The electronic characteristics of the nature of B–N interactions were further studied by Natural Bonding Orbital analysis derived from the theoretically calculated electron densities. This real-space bonding indicator discriminates the bonding B–N contact in **5** from the nonbonding in **8**, which correlates with the flexibility of the naphthyl scaffold to respond to the Lewis acidity of boron allowing shorter peri interactions. Whereas, the steric shielding imposed by the two mesityl groups, and/or the rigidity of the acenaphthene framework disrupt B–N interaction. Thus, this communication reports on the modulation of the B–N bonding continuum by means of structural tuning leading to a molecular switch, as well as its implications towards revealing FLP reactivities through the isolation of intermediates of a stepwise mechanism.

Introduction

Combinations of Lewis acids and Lewis bases have been attracting significant research interest in the field of bifunctional catalysis,^{1,2} and ion sensing.^{3,4} The use of boron in such combinations has been nicely exemplified especially with phosphorous bases. The introduction of a phenyl spacer between the phosphorous and the boron atoms provided π -conjugated donor-acceptor adducts which afforded original small molecule interactions and peculiar bonding situations.^{5–8} The exploration of other structural scaffolds to disrupt this π -conjugation has been achieved by the introduction of a naphthyl spacer inducing marked structural differences (Fig. 1a).^{9,10}

Lately similar constructs have found elegant applications in the development of Frustrated Lewis Pairs (FLPs).^{11–16} The potential of FLPs towards benign metal-free activation of small molecules is revolutionizing the field of catalysis. This concept is based on the notion that combinations of Lewis acids and bases that are prevented from forming classical adducts preserve dual Lewis acidity and basicity, and thus precipitate unexpected reactivity through a cooperative interaction with another molecule.

From the first observation of the facile heterolytical cleavage of hydrogen gas by amines and $B(C_6F_5)_3$,^{17,18} this field is quickly evolving to highly active non-metal catalysts for small-molecule activation. These approaches are expected to bring significant advances in catalysis, including asymmetric versions, while avoiding the requirement of transition metals.^{19,20}

The naphthyl scaffold has been recently involved in the development of new FLPs involving electrophilic phosphonium cations.^{21,22}

Fig 1a. P series (precedent)



Fig 1b. N series (this work)

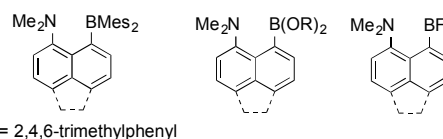


Figure 1. P- and N-Series of 1,8-naphthalenes and 5,6-disubstituted acenaphthenes.

As illustrated by Mebs and Kilian literature precedents on acenaphthylphosphine derivatives,^{9, 23–25} the formal addition of a two-carbon “ace” bridge can induce striking structural

^a Laboratoire de Chimie de Coordination, Centre National de la Recherche Scientifique UPR 8241, 205, Route de Narbonne, F-31077 Toulouse, France.

^b Université Fédérale Toulouse Midi-Pyrénées, 118 Route de Narbonne, F-31062 Toulouse, France.

* Corresponding authors e-mail: emmanuel.gras@lcc-toulouse.fr; Tel.: +33-561-333-1560; fax: +33-561-553-003; pla@lcc-toulouse.fr

Electronic Supplementary Information (ESI) available: Experimental procedures and spectral data, computational analysis, X-ray crystallographic files in CIF format. See DOI: 10.1039/x0xx00000x

effects, which translate into diverse reactivity modulation arising from enforcing/precluding Lewis acid-base pairs interactions. This highlights that minute modifications of structural parameters can be used as a tool to have a rational control over reactivity.

B–N pairs have also found significant developments, especially in the field of FLPs,²⁶ and recent work has clearly illustrated that a modulation of the scaffold and the substituents induces tremendous effects on the nature of the interaction between the donor and acceptor sites.²⁷

Thus our interest in the assemblage of Lewis acids and nitrogen bases in well-defined molecular scaffolds led us to further explore the effects of both the substitution on B, and the implementation of harder bases than phosphorous, aiming to enable switchable intramolecular interactions (*Fig 1b.*). In particular, we were willing to explore the possibility to tweak the interaction by a reversible protonation of nitrogen. This, indeed, offers an advantage towards classical phosphorous systems, where its derivatization renders the quaternization irreversible. Following the seminal contributions of Whiting,²⁸ on dimethylaminoborane adducts for bifunctional catalysis, we decided to expand and further study the advantages conferred by rational structural modifications. Thus, the present study involves the interconversion from naphthyl to acenaphthyl scaffold as a tool to modulate B–N interactions, which has not been thoroughly investigated before.

Moreover, detailed studies of structure-reactivity relationships of these systems by X-ray, NMR and computational methods have been performed to gain further insight into the nature of the B–N interaction, its impact on the molecular architecture as well as its effect on reactivity.

Results and discussion

Pinacolboronates **1** and **2** were respectively obtained from their corresponding brominated precursors by Pd-catalyzed borylation involving bispinacolatodiboron (91%), and Li halogen exchange followed by trapping with methoxy-pinacolborane (50%) (*Fig. 2*).

The quite dissimilar ¹¹B chemical shifts (CDCl₃) of **1** (22.0) and **2** (31.9) gave initial evidence that the bonding situation might be different in this case due to the sole effect of the framework. Whereas, the signal at 31.9 ppm of **2** is indicative of a tricoordinated boronic derivative, the roughly 10 ppm difference in chemical shift of **1** suggested significant pyramidalization of the B center.

To assess the influence of N in this event, we aimed to prevent the interaction of the lone pair of N by generation of ammonium salts **3** and **4**. Therefore, we struggled to find a non-cannonical protocol allowing the protonation of the nitrogen center compatible with the acid-lability of the pinacol ester. The use of methyl triflate in CH₂Cl₂, followed by *tert*-butyl methyl ether (TBME) precipitation of the desired product proved ideal for this purpose avoiding both ester hydrolysis and further *N*-alkylation of the substrate.²⁹

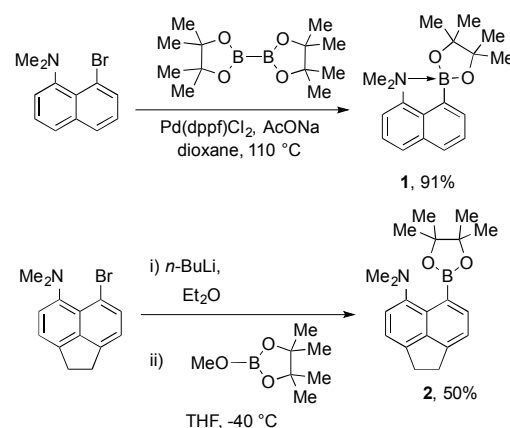


Figure 2. Syntheses of **1** and **2**.

Thus, we were glad to evidence how the ¹¹B chemical shift of the triflate salt **3** (30.5 ppm), almost matched the one of **2** (31.9 ppm). This slight 1.4 ppm difference can be attributed to a modification of the chemical space around boron potentially inducing intramolecular H–bonding interactions as similarly observed for **4** (for which a 1.7 ppm difference is found).

The difference towards fluorination was decisive to assess the scaffold effects on the reactivities of the B and N centers. Despite the known relative instability of aryldifluoroborane species,^{30–32} the strong B–N interaction in the naphthyl series enforces stabilization of **5** (86% yield, *Fig. 3*), as previously reported by Whiting.²⁸ Interestingly, the B–N interaction in difluoroborane **5** is strong enough to prevent protonation and isolation of the corresponding ammonium trifluoroborate adduct. Indeed upon treatment of **5** with an excess of TfOH and KHF₂ such a trifluoroborate could only be transiently observed by ¹¹B NMR together with **5**, but attempts to isolate it only led to decomposition.

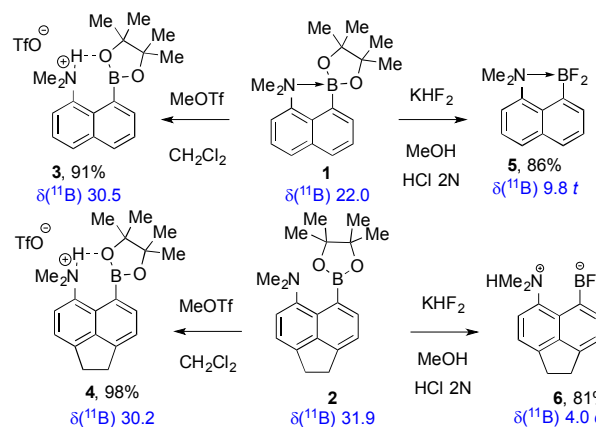


Figure 3. Downstream transformations of **1** and **2**.

Contrarily, the B–N interaction in **1** can be disrupted by protonation of N as observed by ¹¹B NMR upon treatment of **1** with an excess of TfOH (see ESI, page S25). This evidences the stronger character of the B–N interaction in **5** (which correlates with a strong Lewis acidity enhancement).

Alternatively and illustrating the effect of the “ace” bridge, an ammonium trifluoroborate derivative can be efficiently synthesized when the acenaphthene scaffold is in place (**6**, 81% yield).

Pursuing an increase in the Lewis acidity of B in comparison to the boronates **1** and **2**, while sterically shielding B to minimize electronic donation into the vacant orbital, we decided to explore installation of two mesityl substituents on the boron center. Thus, the reaction of 1-bromo-8-(dimethylamino)naphthalene, and 5-bromo-6-(dimethylamino)-acenaphthene, with *n*-BuLi at $-40\text{ }^{\circ}\text{C}$ proceeded with facile metal halide exchange and gave rise to formation of the corresponding lithium organyles which were then reacted with fluorodimesitylborane to yield the corresponding dimesitylborane derivatives **7** (84%) and **8** (55% yield, Fig. 4).

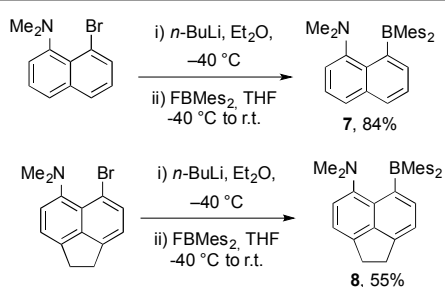


Figure 4. Synthesis of **7** and **8**.

^{11}B NMR analysis of concentrated solutions of **7** and **8** (in CDCl_3) showed only weak signals corresponding to the desired products (68.1, and 74.0 ppm, respectively). Upon protonation of **7** with TFA, the chemical shift of **9** exactly matches that of **8** (74.0 ppm). By removing the electron-density on the N center through formation of the ammonium salt it is possible to disrupt the B–N interaction on this scaffold, as it can be qualitatively measured by ^{11}B NMR. This serves as a threshold to identify the lack of interaction in these systems. Therefore, the ^{11}B chemical shift for **8** was the initial evidence of the acenaphthene scaffold effect on fully precluding the intramolecular donor-acceptor interaction.

The stability of **7** has been assessed towards hydrolysis with 10% solutions of H_2O , HOAc, and $\text{CF}_3\text{CO}_2\text{H}$ in CDCl_3 . **7** remained unchanged under these conditions (Fig. 5).³³ Only stronger acids such as 10% $\text{CF}_3\text{SO}_3\text{H}$ in CDCl_3 triggered decomposition of the starting material.³⁴

Surprisingly, the combination of steric hindrance imposed by the mesityl groups, and the ring torsion due to the acenaphthene scaffold confers a peculiar spatial disposition to **8** regarding water activation (Fig. 5). We hypothesize that this reaction mechanism preferentially occurs via hydrolysis of the C–B bonds, as it has been reported by Hoefelmeyer for 8-(dimesitylboryl)quinolone, Jäkle for (dimesitylboryl)pyridinylferrocene, and Wang for (dimesitylboryl)ferrocenylbenzimidazole.^{35–37} Mechanistic evidence has been obtained through isolation of the borinic acid **10** corresponding to partial hydrolysis of the precursor, as well as the fully

hydrolyzed boronic acid analog **11**, which confirm this reaction path. Moreover, **6** can be prepared by an alternative route starting from **10**. Its peculiar reactivity allows the cleavage of the B–C bond, followed by B–F bond formation to yield **6** (55%, Fig. 5).

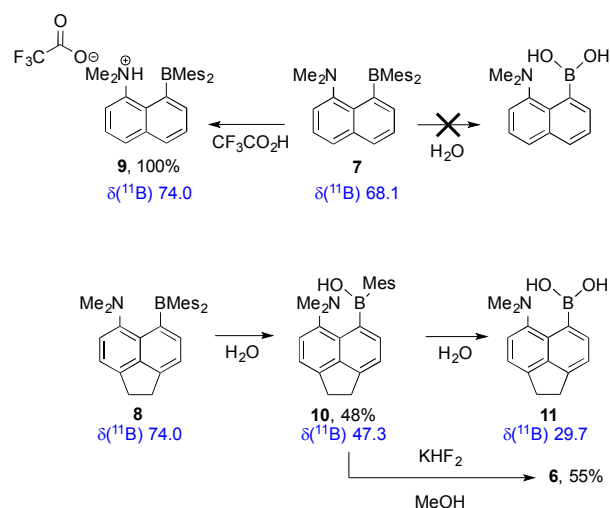


Figure 5. Downstream transformations of **7** and **8**.

The bond situation in related naphthalenes and acenaphthenes has been almost entirely analyzed by inspection of the molecular geometries obtained by X-ray crystallography (Fig. 6), which lead to an unambiguous distinction between bonding and nonbonding peri interactions. These examples suggest that the two atoms in the peri positions can be assorted by attractive and repulsive forces to various degrees. The donating effects towards B can be tuned by the effect of ring torsion on the bicyclic scaffold. Whereas, there is a considerable pyramidalization effect due to B–N interactions throughout the naphthyl series, the influence of the acenaphthene precludes this interaction and the geometries of B remain trigonal planar.

Upon formation of the triflate salt **4**, which further enlarges the B–N distance by 0.462 \AA , the sum of the covalent bond angles around B exactly matches 360.0° , corresponding to a trigonal planar spatial arrangement of B. Thus, the steric congestion imposed by the pinacol ester derivatives is relieved by the N–H \cdots O bond formation in **4** and lower out-of-plane displacements for B and N are observed. This hydrogen bond interaction is thermodynamically favored and confers kinetic stabilization due the topology imposed by the scaffold. Analogous N \cdots H–O hydrogen bond interactions have been observed for **10** and **11**. The higher splay angles (indicative of the angle formed by bonds at peri-positions, see ESI) displayed 22.99 , 18.75° and 20.58 respectively for these compounds may be attributed to the spatial requirements needed to accommodate such H–bonding interactions.³⁸ Thus, this molecular switch encompasses the disruption of the B–N bond, while inducing a significant structural reorganization associated with the formation of a hydrogen bond. Indeed a 94° rotation around the C–B bond is observed in the

acenaphthyl serie together with the formation of an intramolecular H-bond (Fig 7). This structural reorganization is thought to account for the difference in ^{11}B chemical shift mentioned previously between **2** and **4**. The reversibility of the process has been assessed on the basis of ^{11}B chemical shifts (See ESI, page S26).

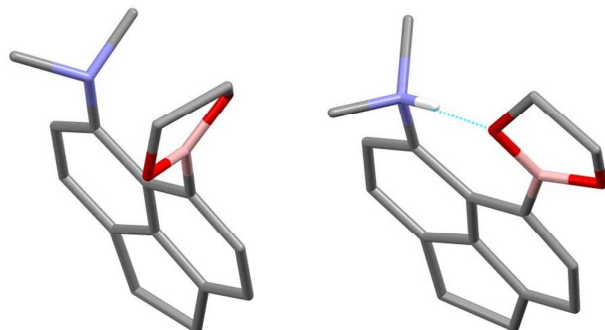


Figure 7. Reversible rotational switch from **2** to **4** (H and Me groups of the pinacol moiety have been removed for the sake of clarity).

The differential behavior of the (ace)naphthyl series towards fluorination also provides an interesting tool to further study the bond topology and the influence of the scaffold in the stabilization of the difluoroborane adduct or trifluoroborate salt derivatives, namely **5** and **6**. In addition, the shorter Van der Waals radius of fluorine translates to a lower steric congestion for **5** and **6** in regard to the parent boronate compounds **1** and **4**, respectively (see ESI page S28 for bond distances). The significant exception to this trend in the naphthyl series is evidenced in **7** by the incorporation of two mesityl substituents on B. The steric bulk imposed by these groups forces the peri-substituents further apart as evidenced by a positive splay angle of 10.24° , and an increased out-of-plane displacement, causing disruption of the B–N interaction to a great extent albeit with a larger out-of-plane displacement. This disruption can be attributed to the harder character of N and its smaller Van der Waals radius. In comparison, the more diffuse nature of the P atom enabled the generation of a B–P interaction over larger distances.¹⁰ Therefore, aminonaphthylboranes display advantageous properties to modulate reactivity in comparison to analogous phosphinonaphthylboranes. Moreover, analogous compound **8** evidences a total disruption of the B–N interaction due to the additive effects of ring torsion provided by the acenaphthene framework (positive splay angle of 15.55°). Natural Bonding Orbital (NBO) analysis has been employed in order to supplement our spectroscopic and crystallographic findings. This method studies the strength of dative bonds taking into account the experimental atomic coordinates obtained by X-ray crystallography. Computational analysis directly revealed a natural B–N orbital to describe the strong interaction present in **5** with almost complete electronic

occupancy ($1.96 e^-$) (See ESI, page S132). For other members of the series (**1**, **2**, **4-8**, **10**, **11**), the strength of the interaction was assessed by donor-acceptor NBO interactions between nitrogen atom lone pair (LP) orbitals and empty boron orbitals by means of second-order perturbation theory analysis. This shows that in the intramolecular B–N dative bonds, interaction is between the LP orbital of the nitrogen atom and a vacant virtual (LV) boron orbital.

Calculated E^2 energies between donor and acceptor orbitals in these dative bonds are given in Table 2. Thus, decreased occupancy in N and increased occupancy in B classifies **1** as the second strongest B–N interaction of the series (164 Kcal/mol), which is in agreement with experimental data. This interaction in the naphthyl series can be greatly disrupted through the incorporation of bulky mesityl groups on boron (**7**, 8.31 Kcal/mol). The acenaphthene framework is a privileged scaffold that precludes this interaction to a higher extent. Thus, the analogous **8** shows the weakest B–N interaction (4.43 Kcal/mol) due to the dual contribution of the acenaphthene ring torsion and steric congestion of both mesityl groups. Lowering the presence of bulky groups on boron translates into a slight increase of the interaction as assessed by the higher electronic occupancies of the boron vacant orbital for **2** (0.38 respectively).

The possibility of H-bonding of the nitrogen atom plays an important role defining these systems as observed by X-ray data. These computational studies bring additional corroboration to this experimental evidence for **4**, **6**, **10**, **11**, and serve to set up the lower limit for no B–N interaction.

Experimental Section

Synthesis: A series of compounds containing dimethylamino and boron groups in the peri positions of a naphthyl scaffold have been prepared and fully characterized. General procedures and detailed experimental descriptions of **1-11** can be found in the ESI.

X-ray Crystallography: The structures were solved by direct methods and refined accordingly. All non-H atoms were refined using anisotropic displacement parameters. H atoms attached to C atoms were included in geometrically calculated positions using a riding model. Crystal and refinement data are collected in the ESI. Crystallographic data have been deposited to the Cambridge Crystallographic Data Centre as CCDC 1403306-1403313. Copies of this information may be obtained free of charge from The Director, CCDC, 12 Union Road, Cambridge CB2 1EZ, U.K. (fax +441223336033, e-mail deposit@ccdc.cam.ac.uk, or www.ccdc.cam.ac.uk/data_request/cif).

Computational studies: NBO analysis was performed with NBO 6.0 implemented in Gaussian09 at the B3LYP/6-31G** level unless otherwise stated. NBO analysis was used to assess the intramolecular dative bond strength.

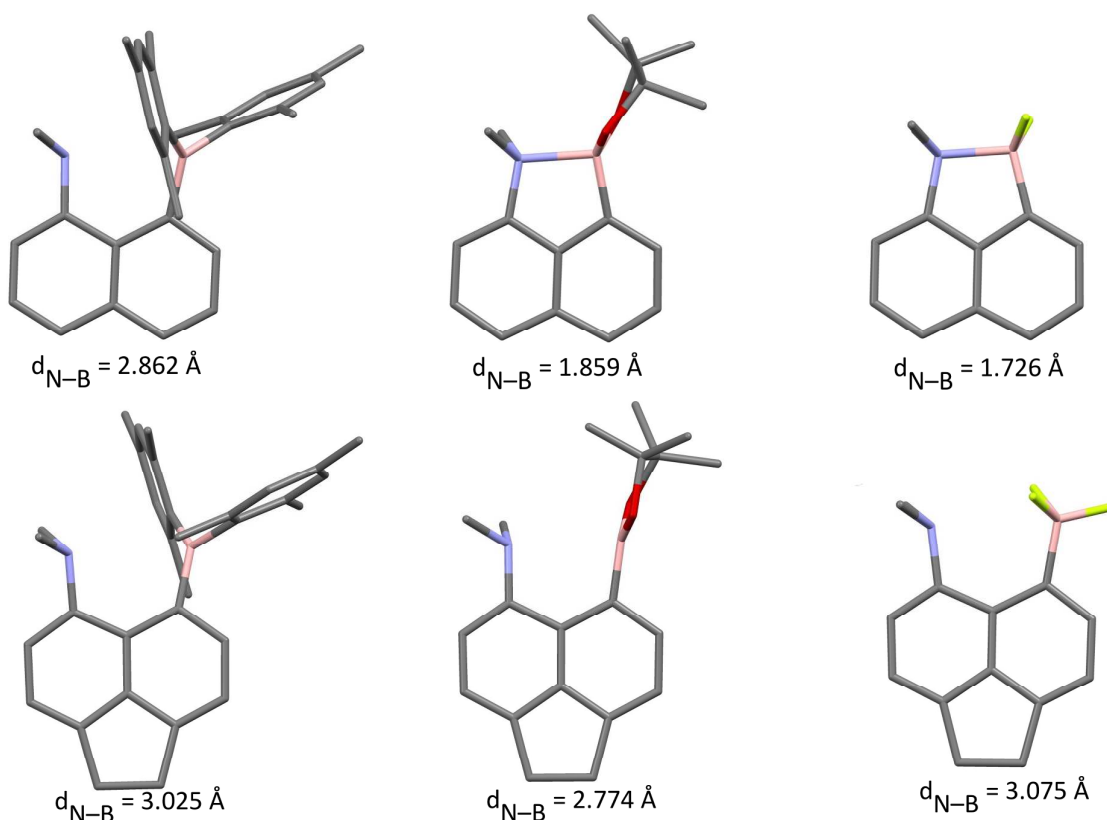


Figure 6: Crystal Structures of selected naphthyl (**1**, **5**, **7**) and acenaphthyl (**2**, **6**, **8**) derivatives and B–N interatomic distances.

The donor-acceptor interaction energy in the NBOs was estimated via second-order perturbation theory analysis of the Fock matrix,³⁹ and establishes the strength of that interaction. For each donor orbital (*i*) and acceptor orbital (*j*), the stabilization energy E^2 is associated with $i \rightarrow j$ delocalization, given by Eq. 1 where q_i is the donor orbital occupancy, $F_{(i,j)}$ is the Fock matrix elements between the NBO *i* and *j*, and ϵ_i and ϵ_j are the orbital energies.

$$E^2 = \Delta E_{ij} = q_i \frac{F_{(i,j)}^2}{\epsilon_i - \epsilon_j}$$

Equation 1. Second-order stabilization energy.

Conclusions

Herein we report the influences imposed by the (ace)naphthyl framework and boron substituents on the B–N bonding continuum and its associated reactivities. The naphthyl scaffold has been found to retain enough flexibility to respond to the Lewis acidity of boron by displaying B–N interaction for the boronic ester **1**, and fluoroborane **5** derivatives ($d_{N-B} = 1.859, 1.726$ Å respectively). Notably, the Lewis pair interaction can be further controlled via the Brønsted basicity of the N center. Thus a simple protonation of the amino group

acts as a reversible trigger promoting a controlled rotation around the C–B bond. On the other hand, the higher steric hindrance of **7** enforces a nonbonding disposition, which allows this compound to be classified as a FLP ($d_{N-B} = 2.862$ Å). Moreover, the rigidity imposed by the acenaphthene framework clearly prevents B–N bonding interactions across all members of the series ($d_{N-B} = 2.774 - 3.236$ Å). Despite their structural similarities, **5** and **8** possess quite different B–N distances of 1.726 and 3.025 Å, respectively, which classifies them as straightforward cases of regular Lewis pairs and FLPs. This classification takes into account the reactivity pattern observed for these compounds. This is exemplified by **8**'s propensity towards water activation and concomitant cleavage of B–C bonds, while other members of the series, namely **7**, display a high stability towards hydrolysis of the C–B bonds in the presence of water and acids. Therefore, the topology and atom disposition present in each of these molecular architectures are crucial factors towards enabling native interactions with other small molecules by bringing novel reactivity modes.

Analysis of a set of Natural Bonding Orbitals derived from the theoretically calculated electron densities confirms the bonding and nonbonding states of the N and B atoms.

Table 2. NBO electronic occupancy and second-order perturbation theory analysis.

Compound	N-B Bond Occupancy	Wiberg Bond Index	Second Order Perturbation Theory Analysis (Kcal/mol)	LP N Occupancy	LV B Occupancy
7	-	0.0909	8.31	1.86136	0.22843
1	-	0.4028	164.20	1.70604	0.41567
5	1.96438	0.4475	-	-	-
8	-	0.0594 ^b	4.43	1.87718	0.21576
10 ^a	-	0.0054	-	1.87329	-
11	-	0.0037	-	1.88481	0.40746
2	-	0.0608	10.88	1.86329	0.38143
4	-	0.0009	-	-	0.42275 ^b
6	-	0.0016	-	-	-

^a NBO analysis shows a double bond between B and O, this can be attributed to the analysis considering the N⁻H=O bond strong enough that it generates the ammonium, therefore forming a pseudo O=B bond. ^b Calculated with 6-31G basis set.

This work demonstrates the significant differences induced by the involvement of N in non- π -conjugated donor acceptor compounds compared to previously reported phosphorous analogues and the influence of the scaffold and boron substituent on the through space interaction between the Lewis acid and the Lewis Base. Further studies towards activation of small molecules with these compounds are currently underway and will be reported in due course.

Acknowledgements

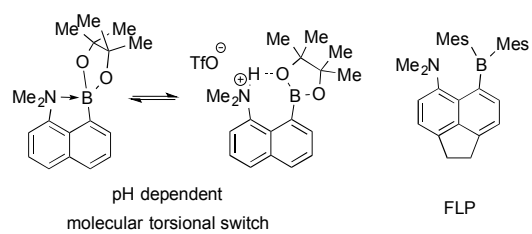
We are grateful to Anaïs Chalard for assistance with the preparation of precursors. We acknowledge Dr Christine Lepetit for valuable discussions regarding the computational part of the work. We are grateful to Dr Rémy Brousses, Dr Carine Duhayon, Dr Laure Vendier, Dr Jean-Claude Daran, and Sonia Mallet-Ladeira for acquiring the X-ray crystallography data at the Laboratoire de Chimie de Coordination. Mass spectrometry data was obtained at the Mass Spectrometry Facility of the Institut de Chimie de Toulouse. Financial support from the French National Agency for Research (Agence National de la Recherche, ANR Blanc, ANR-12-BS07-0005 - BoBo) and the Université Paul Sabatier - French Ministry of Higher Education (Doctoral Fellowship to O.S.) are gratefully acknowledged.

Notes and references

1. A. S. Batsanov, I. Georgiou, P. R. Girling, L. Pommier, H. C. Shen and A. Whiting, *Asian J. Org. Chem.*, 2014, **3**, 470-479.

2. I. Georgiou and A. Whiting, *Org. Biomol. Chem.*, 2012, **10**, 2422-2430.
3. Y. Li, Y. Kang, J.-S. Lu, I. Wyman, S.-B. Ko and S. Wang, *Organometallics*, 2014, **33**, 964-973.
4. C. R. Wade, A. E. Broomsgrove, S. Aldridge and F. P. Gabbai, *Chem. Rev.*, 2010, **110**, 3958-3984.
5. M. Sircoglou, S. b. Bontemps, G. Bouhadir, N. Saffon, K. Miqueu, W. Gu, M. Mercy, C.-H. Chen, B. M. Foxman, L. Maron, O. V. Ozerov and D. Bourissou, *J. Am. Chem. Soc.*, 2008, **130**, 16729-16738.
6. S. Porcel, G. Bouhadir, N. Saffon, L. Maron and D. Bourissou, *Angew. Chem. Int. Ed.*, 2010, **49**, 6186-6189.
7. O. Basle, S. Porcel, S. Ladeira, G. Bouhadir and D. Bourissou, *Chem. Commun.*, 2012, **48**, 4495-4497.
8. R. Declercq, G. Bouhadir, D. Bourissou, M.-A. Légaré, M.-A. Courtemanche, K. S. Nahi, N. Bouchard, F.-G. Fontaine and L. Maron, *ACS Catal.*, 2015, **5**, 2513-2520.
9. J. Beckmann, E. Hupf, E. Lork and S. Mebs, *Inorg. Chem.*, 2013, **52**, 11881-11888.
10. S. Bontemps, M. Devillard, S. Mallet-Ladeira, G. Bouhadir, K. Miqueu and D. Bourissou, *Inorg. Chem.*, 2013, **52**, 4714-4720.
11. D. W. Stephan, *Acc Chem Res*, 2015, **48**, 306-316.
12. A. J. P. Cardenas, Y. Hasegawa, G. Kehr, T. H. Warren and G. Erker, *Coord. Chem. Rev.*, 2015, DOI: 10.1016/j.ccr.2015.01.006.
13. A. Y. Houghton, J. Hurmalainen, A. Mansikkamäki, W. E. Piers and H. M. Tuononen, *Nat. Chem.*, 2014, **6**, 983-988.
14. M. J. Kelly, J. Gilbert, R. Tirfoin and S. Aldridge, *Angew. Chem. Int. Ed.*, 2013, **52**, 14094-14097.
15. O. Ekkert, G. G. Miera, T. Wiegand, H. Eckert, B. Schirmer, J. L. Petersen, C. G. Daniliuc, R. Fröhlich, S. Grimme, G. Kehr and G. Erker, *Chem. Sci.*, 2013, **4**, 2657.
16. Y. Hasegawa, G. Kehr, S. Ehrlich, S. Grimme, C. G. Daniliuc and G. Erker, *Chem. Sci.*, 2014, **5**, 797-803.
17. G. C. Welch, J. D. Masuda and D. W. Stephan, *Inorg. Chem.*, 2006, **45**, 478-480.
18. G. C. Welch and D. W. Stephan, *J. Am. Chem. Soc.*, 2007, **129**, 1880-1881.
19. D. Chen, Y. Wang and J. Klankermayer, *Angew. Chem. Int. Ed.*, 2010, **49**, 9475-9478.
20. L. Shi and Y.-G. Zhou, *ChemCatChem*, 2015, **7**, 54-56.
21. M. H. Holthausen, R. R. Hiranandani and D. W. Stephan, *Chem. Sci.*, 2015, **6**, 2016-2021.
22. M. H. Holthausen, J. M. Bayne, I. Mallov, R. Dobrovetsky and D. W. Stephan, *J. Am. Chem. Soc.*, 2015, DOI: 10.1021/jacs.5b04109.
23. P. Wawrzyniak, A. L. Fuller, A. M. Slawin and P. Kilian, *Inorg. Chem.*, 2009, **48**, 2500-2506.
24. P. Wawrzyniak, A. M. Slawin, J. D. Woollins and P. Kilian, *Dalton Trans.*, 2010, DOI: 10.1039/b916425a, 85-92.
25. B. A. Chalmers, M. Buhl, K. S. Athukorala Arachchige, A. M. Slawin and P. Kilian, *J. Am. Chem. Soc.*, 2014, **136**, 6247-6250.
26. S. Schwendemann, R. Fröhlich, G. Kehr and G. Erker, *Chem. Sci.*, 2011, **2**, 1842.
27. K. Chernichenko, B. Kotai, I. Papai, V. Zhivonitko, M. Nieger, M. Leskela and T. Repo, *Angew. Chem. Int. Ed.*, 2015, **54**, 1749-1753.
28. R. L. Giles, J. A. K. Howard, L. G. F. Patrick, M. R. Probert, G. E. Smith and A. Whiting, *J. Organomet. Chem.*, 2003, **680**, 257-262.

29. Experiments carried out with direct addition of TfOH resulted in total protodeborylation of the starting material. However, water traces in CH₂Cl₂ can account for a slow release of TfOH, which concomitantly protonates the N center while avoiding side reactions.
30. E. Vedejs, R. W. Chapman, S. C. Fields, S. Lin and M. R. Schrimpf, *J. Org. Chem.*, 1995, **60**, 3020-3027.
31. H.-J. Frohn, H. Franke, P. Fritzen and V. V. Bardin, *J. Organomet. Chem.*, 2000, **598**, 127-135.
32. H.-J. Frohn, F. Bailly and V. V. Bardin, *Z. Anorg. Allg. Chem.*, 2002, **628**, 723-724.
33. An analytical sample of **7** (5 mg) was dissolved in CDCl₃-TFA (10:1, 550 μL) in an NMR tube and periodical NMR experiments were run. No traces of decomposition observed by ¹H, ¹³C, and ¹¹B NMR during 7 days time-course.
34. Total decomposition after 20 min of incubation observed by ¹H, ¹³C, and ¹¹B NMR.
35. J. H. Son, M. A. Pudenz and J. D. Hoefelmeyer, *Dalton Trans.*, 2010, **39**, 11081-11090.
36. J. Chen, R. A. Lalancette and F. Jakle, *Chem. Eur. J.*, 2014, **20**, 9120-9129.
37. Y.-L. Rao, T. Kusamoto, R. Sakamoto, H. Nishihara and S. Wang, *Organometallics*, 2014, **33**, 1787-1793.
38. X-ray diffraction for salts **3** and **9** in the naphthyl series could not be acquired, as all attempts to obtain monocrystals were unsuccessful.
39. A. E. Reed, L. A. Curtiss and F. Weinhold, *Chem. Rev.*, 1988, **88**, 899-926.



Boron-nitrogen *peri*-substituted naphthyl scaffolds: Small variations but different behaviours.